INTL JOURNAL OF ELECTRONICS AND TELECOMMUNICATIONS, 2024, VOL. 70, NO. 2, PP. 473-480
Manuscript received November 7, 2023; revised June, 2024. doi: 10.24425/ijet.2024.149568

Extreme learning machine approach on heart abnormalities identification in ECG images

Anandhini Medianty Nababan, Umaya Rhamadhani Putri Nasution, Tito Daniel Pandiangan, Farhad Nadi, Al-Khowarizmi, Rahmat Budiarto, Romi Fadillah Rahmat*

***Abstract*—Heart abnormalities are atypical heart conditions that can lead to chronic heart disease. Heart abnormalities can be severe if not treated directly due to the crucial function of the heart as the blood circulation center. Heart abnormalities cannot be seen with the naked eye so it requires the recording of a heartbeat wave or electrocardiogram (EKG) for the disease to be detected. Therefore, a strategy that uses image processing and artificial neural networks to detect anomalies in the heart is strongly advocated. The proposed methods for feature extraction and identification are Invariant Moments and Extreme Learning Machine respectively. The testing procedure for this research employed a total of 386 ECG images as training data. and 44 ECG images for test data, and the heart condition was classified into 4 classes, namely Atrial Fibrillation, T-Wave, ST-Segment, and normal heart conditions. The test was carried out using 3 choices of extreme learning machine activation functions, namely sigmoidal, sine and hard-lim. The test also applied the parameter of hidden neurons in which amounting to 10, 30, 50, 100 and 500. The system accuracy in identifying heart abnormalities achieved 95.45% by the application of the sigmoid function with the total number of hidden neurons equal to 500.**

***Keywords*—Heart abnormality; Electrocardiogram; Image Processing; Extreme Learning Machine; Invariant Moments**

I. Introduction

HEART is an important organ to pump blood to all parts of the human body. Therefore, heart abnormalities can result in a great risk of death for the patients. The causes of heart disorders are varied from irregular eating patterns, hereditary diseases, and unhealthy lifestyles to the effects of other diseases. Some examples of heart abnormalities are atrial fibrillation, bradycardia, ST segment, T-wave, and many more. Heart abnormality is a disease with difficulties to detect with the naked eye, and it could lead to chronic heart disease. Heart disease has become one of the diseases that become a major cause of human death.

ECG images also categorized as an object for image processing and machine learning, such as in sleep apnea obstruction with classification engine such as Support Vector Machine [1], and ECG sensing scheme using Bayesian [2]. While several studies related to heart abnormalities identification and extreme learning machines have been conducted. One of the studies was to identify heart defects using the signal processing method. The study explained that the signal processing method had been successfully applied to describe the heart condition and can identify abnormalities in the heart [3]. Another study discussed cardiac arrhythmias identification using the Wavelet Transform Techniques combined with probabilistic neural network method with whale optimization algorithm. It achieved an accuracy of 96.97% [4].

Another research implemented Gauss method to identify heart abnormalities. In the study, the obtained line graph pattern was analyzed to determine certain points on the line graph. These points become a comparison in the rule-based knowledge system in finding the heart abnormality. The system accuracy achieved 78.26% [5]. The next research was to classify the types of Parkinson's disease. The proposed feature value retrieval was Particle Swarm Optimization (PSO) and Extreme Learning Machine was chosen as the classification method. It achieved an accuracy of 88.27% [6]. The next research was to identify cardiac arrhythmias using fuzzy clustering [7].

Heart abnormalities can be detected by recording the electrical activity of the heart using an electrocardiograph. The results of electrocardiograph observations are in the form of Electrocardiogram graphs that provide information about the size, shape, capacity, and abnormalities of the heart. The Electrocardiogram graph cannot be read by common people, it requires an expert to determine whether the heart condition is normal or abnormal. Therefore, a system is required to identify abnormalities in the heart.

From the previous studies, the aim of this study is to do image classification of electrocardiogram images with Extreme Learning Machine which has better accuracy, thus it will

This work was supported by Universitas Sumatera Utara TALENTA Research Grant no 139/UN5.2.3.1/PPM/KP-TALENTA/R/2023.

Anandhini Medianty Nababan is with Faculty of Computer Science and Information Technology, Universitas Sumatera Utara, Indonesia (e-mail: nababan.anandhini@usu.ac.id).

Umaya Rhamadhani Putri Nasution is with Faculty of Computer Science and Information Technology, Universitas Sumatera Utara, Indonesia (e-mail: umaya.nst@usu.ac.id).

Tito Daniel Pandiangan is with Faculty of Computer Science and Information Technology, Universitas Sumatera Utara, Indonesia (e-mail: 121402044@students.usu.ac.id).

Farhad Nadi is with School of Information Technology, UNITAR International University, Malaysia (e-mail: farhad.nadi@unitar.my).

Al-Khowarizmi is with Department of Information Technology, Universitas Muhammadiyah Sumatera Utara, Medan, Indonesia (e-mail: alkhowarizmi@umsu.ac.id).

Rahmat Budiarto is with College of Computer Science and Information Technology, Albaha University, Saudi Arabia (e-mail: rahmat@bu.edu.sa)

*Romi Fadillah Rahmat is with Department of Information Technology, Faculty of Computer Science and Information Technology, Universitas Sumatera Utara, Indonesia (*Corresponding Author, e-mail: romi.fadillah@usu.ac.id).

accurately identify which type of heart disease classified into three output such as Atrial fibrillation, ST Segment, and T-Wave. This study and implementation will give initial screening for any health practitioner and improve their manual judgement of the disease. Materials and Methodology

A. Attrial Fibrilation, ST-Segment, and T-Wave

Atrial Fibrillation (AFib) is a common abnormal cardiac condition [8]. The four chambers of the heart have a regular beat in a normal heart, while the atria have an unstable rhythm with AFib [9]. A collection of cells that can be found in the right atrium of the heart are referred to as the sinus node. These cells provide the function of the heart's natural pacemaker. Impulses are normally initiated with each beat of the heart, and it is the sinus node that is responsible for producing those impulses. The impulse will first go via the atria, and then it will pass through the Atrioventricular (NA) Node, which is the junction between the upper and lower chambers of the heart. The ventricles contract in a regular beat as a result of this action, allowing blood to be taken into the heart and pumped out to various regions of the body. The upper chambers of the heart (atria) undergo unstable electrical impulses in Atrial Fibrillation. As a consequence, all regions of the heart will vibrate, causing the Atrioventricular Nodes to be pushed into the ventricles. Figure 1 will show the AFib heart conditions.

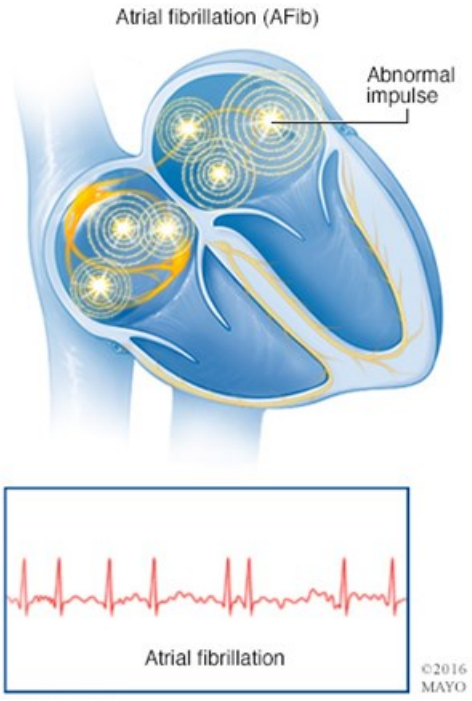

Fig. 1. Atrial Fibrillation ECG Condition [10]

The vast majority of people who suffer from Atrial Fibrillation do not exhibit distinct symptoms and may alone be identified via a physical examination. Common symptoms include tiredness, tachycardia, palpitations, lightheadedness, dyspnea, restlessness, syncope, exertional exhaustion, diaphoresis, and discomfort or a sensation of pressure in the chest region. The following is an example of an ECG image of atrial fibrillation in Figure 2.

Fig. 2. Example of Atrial Fibrillation ECG Image

The time span between the QRS complex and the T wave is known as the ST segment. The ST segment represents the time it takes for the ventricles to go from depolarization to repolarization [11]. The ST segment often displays a level, isoelectric configuration, spanning from the termination of the S wave (JPoint) to the initiation of the T wave. Ischemia and myocardial infarction are the primary causes of significant ST segment abnormalities, which may manifest as either elevation or depression. Figure 3 displays an example of a ST Segment ECG.

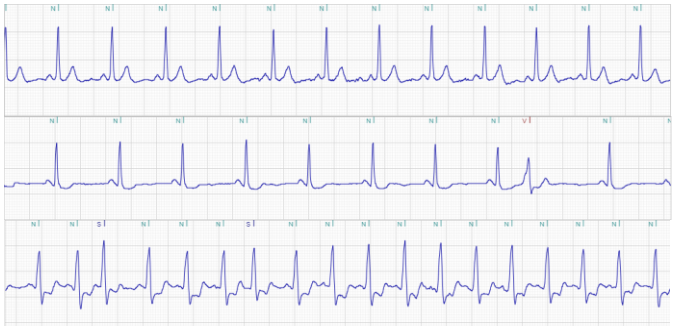

Fig. 3. ST Segment ECG Image.

ST Elevation shown in Figure 4 is an increase in the ST segment above the baseline isoelectric line as measured from the J point (beginning of the end of the QRS complex) [12].

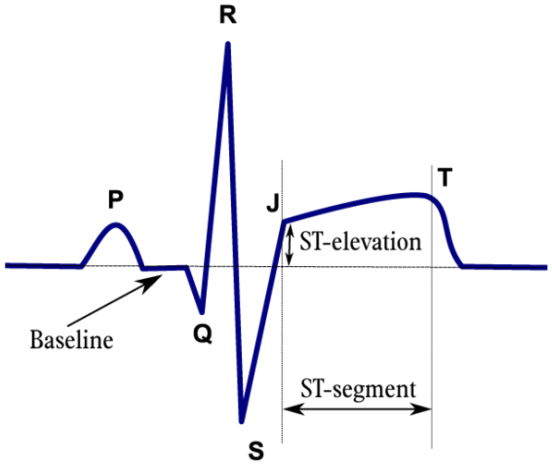

Fig. 4. ST Elevation [13]

ST Depression shown in Figure 5 is a decrease in the ST segment below the baseline isoelectric line as measured from the J point (beginning of the end of the QRS complex) [12].

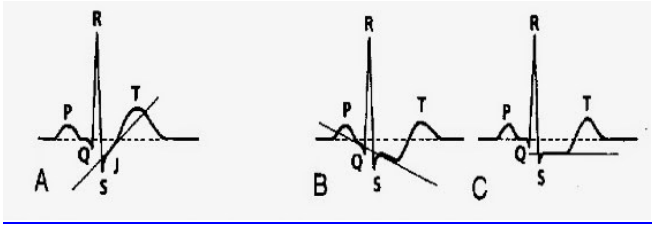

Fig. 5. ST Depression Upsloping (A), Downsloping (B), Horizontal (C)

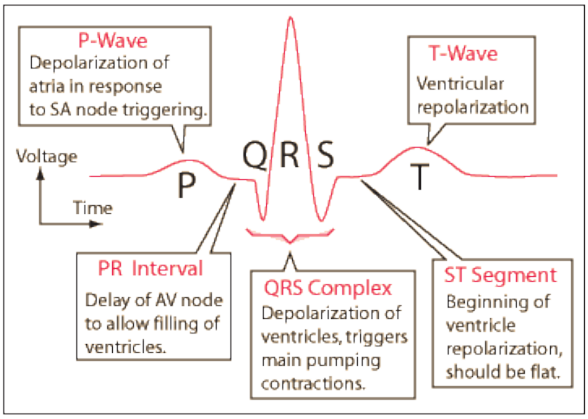

Fig. 6. T-Wave [13]

The T wave is a positive deflection after each QRS wave which has meaning as ventricular repolarization. Characteristics of normal T waves are as follows, positive in all leads except aVR and V1, amplitude generally does not exceed 2/3 of the R wave or < 5 mm in limb leads and < 15 mm in precordial leads [14].

There are several examples of abnormalities that can occur in T waves, namely Tall T Waves or Peaked T Waves which are categorized as Hikperkalemia and Hyperacute T waves (early stages of STEMI) [15]. T-Tall wave abnormalities occur when the T wave pulse is very high and the distance between the T waves is close together, an example of a T-Tall wave abnormality can be seen in Figure 7.

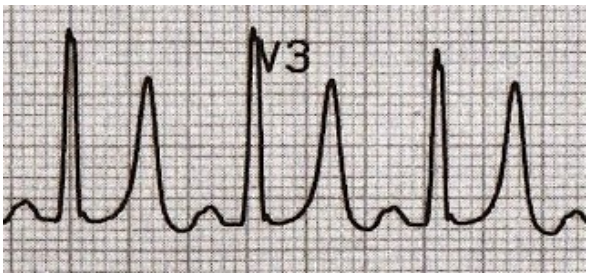

Fig. 7. T-Tall in Hyperkalemia [13]

Another form of T-Wave abnormality is T Wave Inversion. Children often have inverted T wave abnormalities. Inverted T waves manifest when the T wave has a downward deflection, as seen in Figure 2.8 which happen in myocardial infraction, and when the interval between consecutive T waves is very wide.

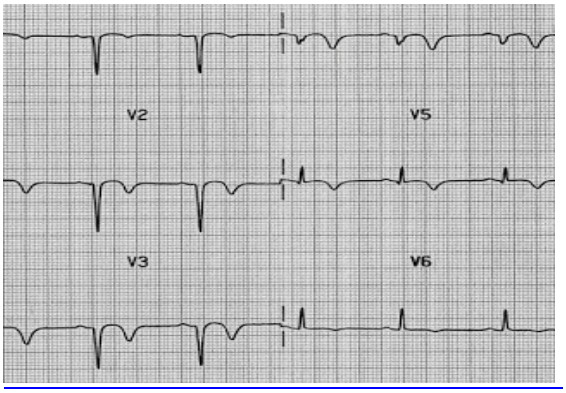

Fig. 8. T-wave inversion in myocardial infarction [13]

Biphasic T wave abnormalities occur if the T wave interval is sometimes upwards and sometimes downwards [15], an example of a Biphasic T wave abnormality can be seen in figure 9.

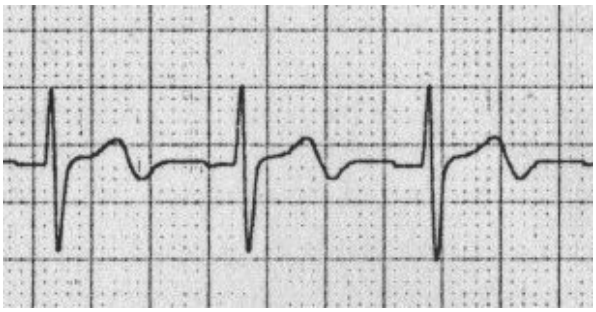

Fig. 9. Biphasic T Waves in Myocardial Ischemia [13]

A camel hump T wave abnormality is seen when the amplitude of the P wave is less than that of the T wave, with the P wave located between the T waves [16]. Figure 2.10 provides an example of such a camel hump T wave abnormality.

Fig. 10. T-waves at 1st degree AV Block [13]

The following is an example of an ECG image with T wave abnormalities taken from Beecardia Physiobank, which can be seen in Figure 11.

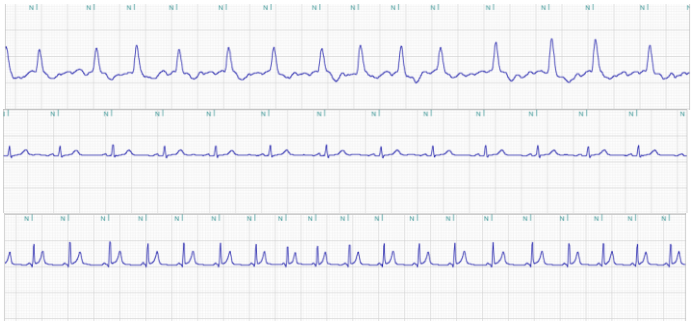

Figure 11. T-Wave ECG Image

B. Dataset

The data used in this study comprises of images sourced from Beecardia physiobank [17] combined with our collected images from Universitas Sumatera Utara Hospital and Adam Malik Hospital. The ECG images displays three cardiac abnormalities, including Atrial Fibrillation, ST Segment deviation, and T-wave abnormalities. However, the overall ECG image indicates a normal functioning heart. The dataset consists of 430 images, each with dimensions of 1000 × 200 pixels. The images are in PNG format. The distribution of the images is shown in Table I.

TABLE I
PARTITIONING OF TRAINING DATA AND TEST DATA

No.	Dataset	Number of Data
1	Training Data	**386**
2	Testing Data	**44**

The acquired images are categorized into two datasets: the training dataset, which will be used to acquire information about numerous forms of cardiac anomalies, and the testing dataset, which will be employed to assess the correctness of the identification procedure. The training dataset comprises 70% of the overall data, while the testing dataset makes up 30% of the total data. The training data includes a total of 386 ECG images, which are categorized into several kinds as shown in Table 2. Here are several instances of electrocardiogram (ECG) images used as a dataset:

TABLE II
NUMBER OF ECG IMAGE TYPES IN THE TRAINING DATA

No.	Heart Abnormalities	Number of Data
1	Attrial Fibrilation	**98**
2	ST-Segment	**83**
3	T-Wave	**109**
4	Normal	**86**

Furthermore, in Table III there are 22 ECG images for testing.

TABLE III
NUMBER OF ECG IMAGE TYPES IN THE TEST DATA

No.	Heart Abnormalities	Number of Data
1	Attrial Fibrilation	**12**
2	ST-Segment	**12**
3	T-Wave	**12**
4	Normal	**8**

C. General Architecture

The general architecture to classify heart abnormalities consists of several stages. These stages begin with collecting normal image data, atrial fibrillation, st-segment, and t-wave to be used for training and test images, the preprocessing stage comprises of resizing to convert the input image size to a size of 1000 x 200 pixels. The data would go to segmentation by forming a binary image using Thresholding then continue to feature extraction process to determine the feature values using Invariant Moments. The results of this process were in the form of seven moment values. These moment values will be set as the input values for the identification process. The last step would be classification using the Extreme Learning Machine. After these steps are carried out, the identification results of the heart abnormalities will be obtained. Figure 12 presents a diagrammatic overview of the overall structure of our investigation.

D. Pre-processing

At this step, the goal is to create an image with a higher quality so that it may be processed at the subsequent stage. The ECG images will be resized to a size of 1000 x 200 pixels.

E. Segmentation

The next step is segmentation, which will be used in conjunction with thresholding to generate a binary image. The objective of this step is to transform the image itself into a binary representation, which is also known as the binary process. The pixel value was changed to either black or white as a result of this operation, which applied a threshold value. The thresholding procedure produced the results of which can be seen in Figure 14.

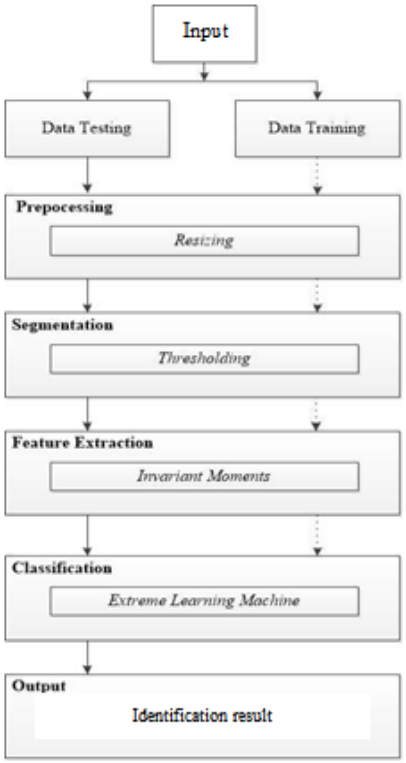

Fig. 12. General architecture

Fig. 14. Threshold result

F. Feature Extraction

The next stage would be feature extraction to extract the feature value from the threshold images using the Invariant Moments method.

The invariant moment is a method to extract shape features in image processing [7]. The results of this method are seven moment values for each image object. These values are independent of translation, rotation, and scaling. The moment value is calculated using (1):

$$m_{pq} = \sum_{x=0}^{H-1} \sum_{y=0}^{W-1} x^p y^p f(x,y) \quad (1)$$

After the moment value was obtained, the process continued with the calculation of the central moment value using (2):

$$\mu_{pq} = \sum_{x=0}^{H-1} \sum_{y=0}^{W-1} (x-\overline{x})^p (y-\overline{y})^q f(x,y) \quad (2)$$

Then, normalization will be carried out using (3):

$$\eta_{pq} = \frac{\mu_{pq}}{\mu_{00^\gamma}} \quad (3)$$

The last step is to calculate the value of invariant moments (ϕ) because the obtained value would be too small to process so they are defined into an equation of $|\log(|\phi|)|$ so that the difference between each value can be significant:

$$\phi_1 = \eta_{20} + \eta_{02}$$

$$\phi_2 = (\eta_{20} - \eta_{02})^2 + 4\eta_{11}^2$$

$$\phi_3 = (\eta_{30} - 3\eta_{12})^2 + (3\eta_{21} + \eta_{03})^2$$

$$\phi_4 = (\eta_{30} + \eta_{12})^2 + (\eta_{21} + \eta_{03})^2 \quad (4)$$

$$\phi_5 = (\eta_{30} - 3\eta_{12})(\eta_{30} + \eta_{12})[(\eta_{30} + \eta_{12})^2 - 3(\eta_{21} + \eta_{03})^2] + (3\eta_{21} - \eta_{03})(\eta_{21} + \eta_{03})[3(\eta_{30} + \eta_{12})^2 - (\eta_{21} + \eta_{03})^2]$$

$$\phi_6 = (\eta_{20} - \eta_{02})[(\eta_{30} + \eta_{12})^2 - (\eta_{21} + \eta_{03})^2] + 4\eta_{11}(\eta_{30} + \eta_{12})(\eta_{21} + \eta_{03})$$

$$\phi_7 = (3\eta_{21} - \eta_{03})(\eta_{30} + \eta_{12})[(\eta_{30} + \eta_{12})^2 - 3(\eta_{21} + \eta_{03})^2] - (\eta_{30} - 3\eta_{12})(\eta_{21} + \eta_{03})[3(\eta_{30} + \eta_{12})^2 - (\eta_{21} + \eta_{03})^2]$$

By applying (4), seven moment values will be generated to be the input values for the Extreme Learning Machine to identify heart abnormalities.

G. Classification

Extreme Learning Machine is the approach that is suggested to be used for the classification process in this investigation. The Extreme Learning Machine, often known as ELM, is a kind of artificial neural network that engages in supervised learning like other types of neural networks [18]. The Feed-Forward Neural Network incorporates ELM and consists of a solitary hidden layer [19]. The ELM technique is thought to effectively address the issue of slow learning seen in other approaches within Feed-Forward Neural Networks [20]. According to their analysis, there are two factors contributing to the slow learning pace of Feed-Forward Neural Networks: the feed The training phase of Forward Neural Networks is conducted using the Slow Gradient Based Learning Algorithm. Furthermore, all parameters in the network are established in an iterative process utilizing this learning mechanism. The factors mentioned here are the input weight and hidden bias, which are interconnected across layers. This interconnection causes the learning process to be prolonged and increases the likelihood of encountering local minimums, resulting in the model being stuck. [20]. Meanwhile, ELM is able to train quickly and provide effective results since the input weight and hidden bias are selected at random [21]–[23]. Randomly generated weights are the key to the success of ELM compared to generating weights from an iterative learning process such as gradient decent [24]. The general architecture of Extreme Learning Machine is shown in Fig. 3.

ELM employs the notion of inverse matrices in the process of learning. The employed theory is the Moore Penrose Pseudoinverse. Figure 3 depicts a basic representation of Single-hidden Layer Feedforward Networks (SLFNs), which serves as the fundamental framework for ELM. This artificial neural network achieves optimal generalization outcomes while maintaining quick computational efficiency. The ELM network architecture has an input layer, a hidden layer, and an output layer. ELM has distinct qualities in comparison to several other artificial neural network techniques. The aforementioned attributes encompass the learning process is very efficient and rapid. One benefit of ELM is its efficiency in learning patterns, even in basic applications, compared to other artificial neural networks that need a longer period time of execution.

ELM achieves greater generalization than gradient-based algorithms like the backpropagation algorithm. Several issues typically arise in gradient-based algorithms, such as inappropriate learning rates, etc. ELM employs additional methods, such as the early halting method, to circumvent these issues.

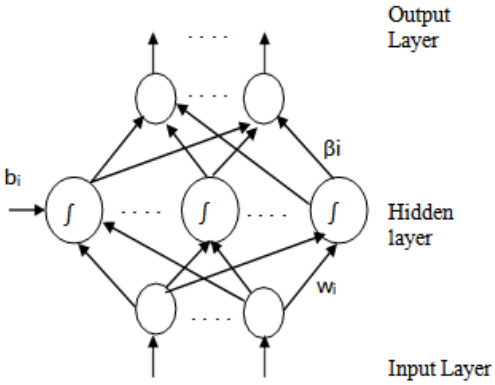

Fig. 3. ELM general architecture

In Extreme Learning Machine, if there are N samples (x_i, t_i) with $x_i = [x_{i1}, x_{i2}, \dots, x_{in}]\ T \in R_n$ and $t_i = [t_{i1}, t_{i2}, \dots, t_{in}] T \in R_n$, then standard SLFN with N hidden neurons and activation function g(x) is defined as:

$$\Sigma_{i=1}^{N}\beta_i g(w_i.x_j + b_i) = 0_j, j = 1, \ldots.., N \qquad (2.5)$$

Where $w_i = [w_{i1}, w_{i2}, \ldots, w_{in}]\ T$ is considered equal to zero, but the size of the vector that connects the hidden neuron with the input neuron appears as defined by $\beta_i = [\beta_{i1}, \beta_{i2}, \ldots, \beta_{in}]\ T$ and b_i is the threshold of the hidden neuron. Tanda "." In $w_i.x_j$ shows the dot product of w_i and x_j. SLFN will shrink the difference between o_j and t_j. So the previous mathematical equation can be written as follows:

$$\Sigma_{i=1}^{N}\beta_i g(w_i.x_j + b_i) = t_j, j = 1, \ldots.., N \qquad (2.6)$$

The mathematical equation above can be converted into matrix form $H\beta = T$ where:

$$\begin{bmatrix} g(w1, x1 + b1) & \cdots & g(wg, xg + bg) \\ \vdots & \ddots & \vdots \\ g(w1, x1 + b1) & \cdots & g(wg, xg + bg) \end{bmatrix}$$

$$H(a_1, \ldots, a_N, b_i, \ldots, b_N, x_1, \ldots, x_N) = N * N \qquad (2.7)$$

$$\beta = \begin{bmatrix} \beta_1^T \\ \vdots \\ \beta_N^T \end{bmatrix} N * m \qquad (2.8)$$

$$\text{and } T = \begin{bmatrix} t_1^T \\ \vdots \\ t_N^T \end{bmatrix} N * m \qquad (2.9)$$

Matrix H represents the matrix of output values from the hidden layer in the artificial neural network. If the number of artificial neuron in the hidden layer is equal to the number of samples, then the matrix H will exhibit symmetry. If the system equations cannot be solved analytically, numerical techniques must be used. Specifically, the following equations are utilized:

$$Min_{\beta}\|H\beta - T\| \qquad (2.10)$$

In order to get optimal results during the training phase, it is important to minimize errors, choose the lowest vector size that offers the highest generalization performance, and ultimately obtain the minimal solution $H\beta = T$

The output consists of 4 nodes (Atrial Fibrillation, Wave T, Segment-ST, and Normal) while the hidden neuron is determined randomly through several trials of system requirements. In this study, the hidden neurons were set to 10, 30, 50, and 100 to determine the best-hidden neuron value to identify abnormalities in the heart.

H. Hyperparameter Setup

A non-optimal number of nodes in the hidden layer may cause problems during training. Insufficient nodes in hidden layers may result in underfitting, in which the available nodes are unable to detect signals received from the input layer properly. On the other hand, having too many nodes may cause the artificial neural network to take longer to process information. Aside from that, having too many nodes may result in overfitting, where the amount of information received is inadequate to be handled in training owing to the network's massive information processing power. Applying the following principles allows one to arrive at an estimate of the number of neurons present in the hidden layer: a value that is greater than the value allocated to the number of neurons in the input layer but lower than the value assigned to the number of neurons in the output layer has to be assigned to the number of neurons in the hidden layer; The number of neurons in the hidden layer cannot have a value that is greater than twice the value of the neurons in the input and output layers combined. Additionally, the number of neurons in the hidden layer cannot have a value that is less than half the value of the neurons in the input and output layers combined.

Rules regarding the number of neurons in the hidden layer can be used as a consideration. However, the process of determining the number of neurons in the hidden layer is a trial-and-error process. This is done so that the network can adapt to the problem to be solved.

For the purpose of this investigation, the training method will be carried out using a variety of different values for the number of neurons in the hidden layer, which will be designated by the symbol n and will vary from 1 to 100. This is done to find the optimum number of neurons that should be in the hidden layer in order to carry out the prediction procedure.

After determining the number of neurons in the hidden layer, the next step is to choose the activation function that will be used by the neurons throughout the training and testing phases. The activation functions used in this study are the sigmoid, sine, and hard-lim functions.

The first phase of the training procedure in this study was assigning input weight and bias values. The number of neurons in the input layer is dynamically set to match the number of parameters acquired from the dataset used in this study. The initial weight and bias of the artificial neural network in this research were randomly assigned.

After the previous step of randomization for the input weights and biases has been finished, the calculation of the hidden layer output matrix is the next phase that must be completed. The output matrix of the hidden layer is the result of the input processing carried out by the neurons in the hidden layer. These neurons get their input from the neurons that make up the input layer. The activation function that was developed in the phase before this one is used in the processing that is carried out.

The computation of the output weight is performed after the process of calculating the output matrix of the hidden layer has been finished. The outcome of this procedure is a matrix that signifies the magnitude of each neuron in the output layer.

II. RESULT AND DISCUSSION

At this stage, the data and system will be tested. Data testing was carried out on 12 atrial fibrillation images, 12 st-segment images, 12 t-wave images, 8 normal images, while training data are 98 atrial fibrillation images, 83 st-segment images, 109 t-wave images, and 86 normal images.

The test was carried out using different Hidden Neuron values, starting from 10, 30, 50, 100, and 500 using 3 activation functions of the extreme learning machine, namely sigmoid, sine and hard-lim. The testing with different Hidden Neuron values aims to get the best value of Hidden Neuron and the activation function to identify heart abnormalities well.

The result of heart abnormalities identification using the sigmoid function is shown in Fig. 5.

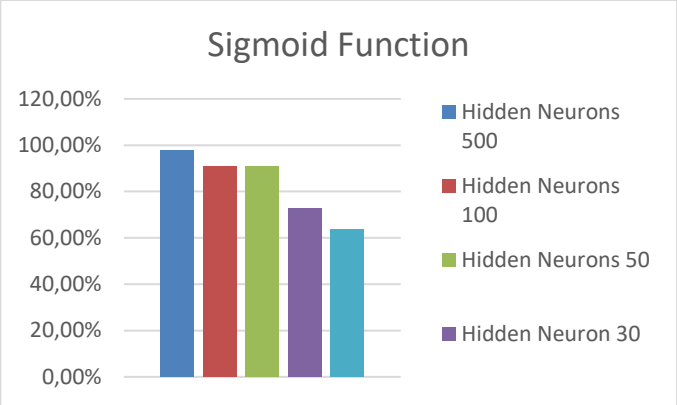

Fig. 5. Accuracy result using sigmoid function

Based on Fig. 5, when the number of hidden neurons given were 50 and 100, it achieved an accuracy result of 90.9% based on 4 false classification images and 40 true images, while with hidden neurons of 10 and 30, the accuracy results were 63.63% (28 true classified images and 16 false classified images) and 72.27% (based on 32 true classified images and 12 misclassified images) respectively using sigmoid as the activation function. For the best accuracy is taken with 500 hidden neurons with 95.45% accuracy result. It is produced from 42 true images with 2 false classification images detected in the system. Those 2 false classifications are misclassification from observed Segment-ST and Wave-T heart abnormalities classified as predicted Normal images.

The result of heart abnormalities identification using the sine function is shown in Fig. 6

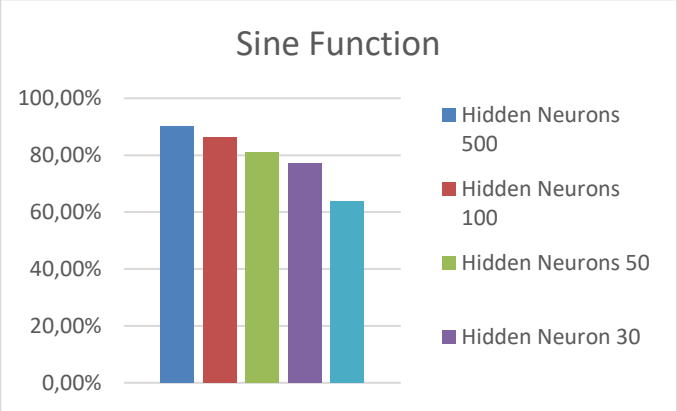

Fig. 6. Accuracy result using sine function

Based on Fig. 6, the best accuracy was obtained when the number of hidden neurons given was 500, it achieved an accuracy result of 90.90%, which resulted from 40 true classified images and 4 false misclassified images. while with hidden neurons 10 30, 50, and 100 the accuracies were 63.63%, 77.27%, 81.81% and 86.36% respectively while using sine as the activation function.

The result of heart abnormalities identification using the hardlim function is shown in Fig. 7. Based on Fig. 7, the best accuracy is obtained when the number of hidden neurons given was 500, it achieved an accuracy result of 88.63% based on 39 correct classification images and 5 misclassification images, while with hidden neurons 10 30, 50, and 100 the accuracy rates were 56.81%, 63.63%, 72.27% and 81.81% respectively while using hardlim as the activation function. ELM with hard-lim activation function is the worst if compared to sigmoid and sine activation function.

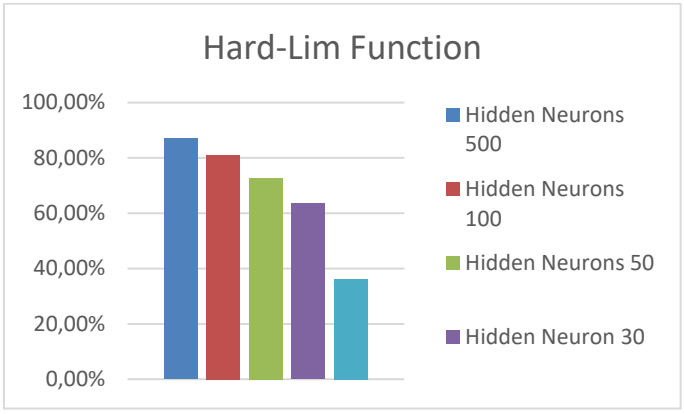

Fig.7. Accuracy result using hard-lim function.

As a result of the examination of Figures 5, 6, and 7, it is possible to draw the conclusion that increasing the number of hidden neurons results in an increase in the accuracy with which cardiac issues are detected.

To get optimal accuracy for each function, it is recommended to use 500 hidden neurons. When using the sigmoid function, the accuracy rate reaches 97.7%. The sine function yields an accuracy of 90.3%, while the hard-lim function results in an accuracy of 87%. The sigmoid function is superior at detecting cardiac problems from ECG image, whereas the hard-lim function has the lowest accuracy among the three functions used in the identification procedure.

If we look at the results obtained and also the number of misclassified images, it can be seen that the misclassified images have similarities between heart abnormalities. It is interesting to see based on the results obtained that the classification for normal heart is quite accurate and there is no misclassification category with existing heart abnormalities. This happens in all results with sigmoid, sine or hard-lim functions applied.

CONCLUSION

Several inferences and conclusions have been reached as a result of the test that was performed to discover heart abnormalities problems using ECG images. Using the sigmoid activation function and setting the parameter configuration of the hidden neurons to 500, the Extreme Learning Machine approach is able to diagnose cardiac problems with an accuracy result of 95.45%. This is made possible by the fact that the system achieves such a high level of precision. Invariant moments are also a good feature recognition method for taking feature values from thresholding images.

The testing of the system allows for the additional conclusion that the number of hidden neurons has an effect on the identification process; specifically, that the system accuracy improves in proportion to the number of hidden neurons that are provided. Additional research may be made by adding various technique combinations in the feature extraction step to achieve more accurate feature values for training data and test data. This can be done to improve the overall accuracy of the model. It is also advised that a better image processing procedure be used,

as this will allow the image segmentation to provide better results by getting rid of other items in their entirety. A greater accuracy rate is another benefit that might arise from having access to more training data.

REFERENCES

[1] "Detection of Obstructive Sleep Apnea from ECG Signal Using SVM Based Grid Search," *International Journal of Electronics and Telecommunications*, Jul. 2023, doi: https://doi.org/10.1680/jsmic.22.00028.

[2] V. Upadhyaya and M. Salim, "Modified Block Sparse Bayesian Learning-Based Compressive Sensing Scheme for EEG Signals," *International Journal of Electronics and Telecommunications*, Jul. 2023, doi: https://doi.org/10.24425/ijet.2021.135985.

[3] V. Rama, C. B. R. Rao, and N. Duggirala, "Analysis of Signal Processing Techniques to Identify Cardiac Disorders," *International Journal of Innovative Research in Electrical, Electronics, Instrumentation and Control Engineering*, vol. 3, no. 6, 2015, doi: http://dx.doi.org/10.13140/RG.2.1.2445.9922.

[4] Li, N., He F., Ma W., Wang R., Jiang L., Zhang X, "The Identification of ECG Signals Using Wavelet Transform and WOA-PNN," in *Sensors*, 2022, 22(12), 4343, https://doi.org/10.3390/s22124343

[5] Saparudin, E. Ramadhan "Heart abnormalities classification using Gauss Method," *Jurnal Generic*, vol 5, no 1, 2010. https://repository.unsri.ac.id/23377/1/5-Saparudin.pdf

[6] M. K. Shahsavari, H. Rashidi, and H. R. Bakhsh, "Efficient classification of Parkinson's disease using extreme learning machine and hybrid particle swarm optimization," in *2016 4th International Conference on Control, Instrumentation, and Automation (ICCIA)*, IEEE, Jan. 2016, pp. 148–154. doi: https://doi.org/10.1109/ICCIAutom.2016.7483152.

[7] N. Joshy and D. Pamela, "Heart Diseases Identification System Using Fuzzy Cluster Algorithm," *International Journal of Engineering Research & Technology (IJERT)*, vol. 03, no. 03, pp. 1217–1220, Mar. 2014. doi: htpps://doi.org/10.17577/IJERTV3IS031095

[8] C. Slovis, "ABC of clinical electrocardiography: Conditions not primarily affecting the heart," *BMJ*, vol. 324, no. 7349, pp. 1320–1323, Jun. 2002, doi: https://doi.org/10.1136/bmj.324.7349.1320.

[9] P. A. Chousou, R. Chattopadhyay, V. Tsampasian, V. S. Vassiliou, and P. J. Pugh, "Electrocardiographic Predictors of Atrial Fibrillation," *Medical Sciences*, vol. 11, no. 2, p. 30, Apr. 2023, doi: https://doi.org/10.3390/medsci11020030.

[10] "Atrial Fibrillation – Symptoms Causes." Accessed: Jun. 17, 2022. [Online]. Available: https://mayoclinic.org

[11] S. B. Eysmann, F. E. Marchlinski, A. E. Buxton, and M. E. Josephson, "Electrocardiographic changes after cardioversion of ventricular arrhythmias.," *Circulation*, vol. 73, no. 1, pp. 73–81, Jan. 1986, doi: https://doi.org/10.1161/01.CIR.73.1.73.

[12] I. Campero Jurado, A. Fedjajevs, J. Vanschoren, and A. Brombacher, "Interpretable Assessment of ST-Segment Deviation in ECG Time Series," *Sensors*, vol. 22, no. 13, p. 4919, Jun. 2022, doi: https://doi.org/10.3390/s22134919.

[13] "ST Segment." Accessed: Jun. 20, 2022. [Online]. Available: https://ina-ecg.com

[14] L. A. Walder and D. H. Spodick, "Global T wave inversion," *J Am Coll Cardiol*, vol. 17, no. 7, pp. 1479–1485, Jun. 1991, doi: https://doi.org/10.1016/0735-1097(91)90635-M.

[15] D. Azab, M. Zahran, and A. Elmahmoudy, "Initial T wave morphology in the chest leads in patients presenting with anterior ST-segment elevation myocardial infarction and its correlation with spontaneous reperfusion of the left anterior descending coronary artery," *International Journal of the Cardiovascular Academy*, vol. 5, no. 2, p. 52, 2019, doi: https://doi.org/10.4103/IJCA.IJCA_1_19.

[16] A. Yong JK, N. JXT, and R. Linch, "Camel Hump T waves and the Tee Pee sign electrocardiographic evidence of severe electrolyte abnormalities," *Emerg Med Investig*, vol. 3, no. 3, Apr. 2017, doi: https://doi.org/10.29011/2475-5605.000040.

[17] "Physiobank." Accessed: Oct. 24, 2023. [Online]. Available: https://beecardia.com

[18] S. Decherchi, P. Gastaldo, A. Leoncini, and R. Zunino, "Efficient Digital Implementation of Extreme Learning Machines for Classification," *IEEE Transactions on Circuits and Systems II: Express Briefs*, vol. 59, no. 8, pp. 496–500, Aug. 2012, doi: https://doi.org/10.1109/TCSII.2012.2204112.

[19] Z.-L. Sun, T.-M. Choi, K.-F. Au, and Y. Yu, "Sales forecasting using extreme learning machine with applications in fashion retailing," *Decis Support Syst*, vol. 46, no. 1, pp. 411–419, Dec. 2008, doi: https://doi.org/10.1016/j.dss.2008.07.009.

[20] G.-B. Huang, Q.-Y. Zhu, and C.-K. Siew, "Extreme learning machine: Theory and applications," *Neurocomputing*, vol. 70, no. 1–3, pp. 489–501, Dec. 2006, doi: https://doi.org/10.1016/j.neucom.2005.12.126.

[21] M. Tiwari, J. Adamowski, and K. Adamowski, "Water demand forecasting using extreme learning machines," *Journal of Water and Land Development*, vol. 28, no. 1, pp. 37–52, Mar. 2016, doi: https://.doi.org/10.1515/jwld-2016-0004.

[22] B. Yadav, S. Ch, S. Mathur, and J. Adamowski, "Assessing the suitability of extreme learning machines (ELM) for groundwater level prediction," *Journal of Water and Land Development*, vol. 32, no. 1, pp. 103–112, Mar. 2017, doi: https://doi.org/10.1515/jwld-2017-0012.

[23] R. F. Rahmat, A. B. Pangaribuan, E. Suwarno, and T. Z. Lini, "Lake Toba Water Quality Prediction using Extreme Learning Machine," *ICIC Express Letters, Part B: Applications*, vol. 13, no. 1, pp. 89–97, 2022. doi: https://doi.org/10.24507/icicelb.13.01.89

[24] F. Mercaldo, L. Brunese, F. Martinelli, A. Santone, and M. Cesarelli, "Experimenting with Extreme Learning Machine for Biomedical Image Classification," *Applied Sciences*, vol. 13, no. 14, p. 8558, Jul. 2023, doi: https://doi.org/10.3390/app13148558.